Macromolecules
ARTICLE

Macromolecules **2009**, *42*, 5027–5035 **5027**
DOI: 10.1021/ma900356p

Formation Efficiency of ABA Blockcopolymers via Enhanced Spin Capturing Polymerization (ESCP): Locating the Alkoxyamine Function

Thomas Junkers,*,† Edgar H. H. Wong,†,‡ Martina H. Stenzel,‡ and Christopher Barner-Kowollik*,†

†*Preparative Macromolecular Chemistry, Institut für Technische Chemie und Polymerchemie, Universität Karlsruhe (TH)/Karlsruhe Institute of Technology (KIT), Engesserstrasse 18, 76128 Karlsruhe, Germany, and* ‡*Centre for Advanced Macromolecular Design, School of Chemical Sciences and Engineering, The University of New South Wales, Sydney, NSW 2052, Australia*

Received February 17, 2009; Revised Manuscript Received May 18, 2009

ABSTRACT: Enhanced spin capturing polymerization (ESCP) constitutes a versatile method for controlling the molecular weights during free radical macromolecular growth. The methodology employs nitrones as controlling agents, which are incorporated as alkoxyamines into the macromolecules in a midchain position (R_i-NO-R_j). It is demonstrated—via both simulations and experiments—that if the radical initiator and the nitrone are judiciously chosen, midchain functionalizations of over 90% can be achieved. Macromolecules with a nitroxide position in the midchain position can be employed in subsequent nitroxide mediated polymerizations to prepare ABA-type block copolymers. It is demonstrated that high yields of midchain macroalkoxyamine are generated as long as the employed nitrone displays low primary radical addition (governed by the addition rate coefficient k_{ad}) in combination with a relatively rapid chain growth initiation rate (characterized by the primary radical initiation rate coefficient, k_i). The absolute value of k_{ad} appears to be unproblematic for the success of R_i-NO-R_j formation by ESCP. In addition, it is of relatively high importance to employ a large nitrone concentration to achieve high degrees of R_i-NO-R_j. The structure of ESCP prepared polystyrenes was confirmed (among other approaches) via thermally cleaving the R_i-NO-R_j species and a subsequent quenching of the reaction to obtain a high yield of the individual arm species of half the length of the macroalkoxyamine.

Introduction

A broad range of procedures can be found in the toolbox of a radical polymerization chemist for designing synthetic routes toward well-defined complex macromolecular architectures.[1,2] Depending on the target structure, sophisticated methods must often be employed that require a comparatively high level of synthetic skills and are thus not easily carried out, especially in industrial contexts. For this reason, new methods are continuously developed to find simpler, more cost-effective, and generally less system specific techniques, which is especially important for the development of commercial applications making use of complex polymers. Recently, we introduced the method of enhanced spin capturing polymerization (ESCP)[3,4] as a simple approach to produce functional polymers with controlled molecular weight in a broad range of reaction media on the basis of our former development of thioketone-mediated polymerization (TKMP)[5−8] and laser induced marking of polymer chains in pulsed laser polymerization experiments.[9] ESCP is not a living polymerization technique; the process does not result in a linear growth of the individual macromolecules. Nevertheless, the polymerizations display excellent molecular weight control by variation of the controlling agent concentration (i.e., nitrones, see below) and—as will be the main focus of the present contribution—carry an alkoxyamine functionality in the *midchain* location of the generated polymer. As consequence, ESCP-derived polymers may be employed as macroinitiators for nitroxide-mediated polymerization (NMP)[10] and thus be converted into a living polymerization system by simply changing the reaction conditions (ESCP is carried out under conventional free-radical polymerization conditions, i.e. temperatures well below 100 °C, while NMP mostly requires the use of elevated temperatures).[11] Nitrones have been used previously in radical polymerization systems, most notably by Detrembleur and Jêrome, who employed these species to form macronitroxides in situ for subsequent NMP reactions.[12−14] The findings of these colleagues during the in situ macronitroxide formation phase are in excellent agreement with recent results from our group.

The ESCP process follows a simple reaction mechanism. Free radicals, mostly propagating macromolecular chains, react with a nitrone forming a stable radical spin trap adduct of the nitroxide type as shown in Scheme 1. These macronitroxides do not persist for a long time in the polymerization, as they are rapidly quenched by propagating chains present in the reaction solution. The initial concentration of the nitrone thereby determines the formed molecular weight of the generated macromolecules as the spin annihilation events are in direct competition with the propagation reaction. As the nitroxides are formed in situ, only moderate steady-state concentrations of spin adducts are formed,[15] thus preventing the complete inhibition of the polymerization as would occur if nitroxide radicals were added to the solution prior to reaction.

We have previously analyzed the influence of some structural elements within nitrones on the specific addition rate coefficient, $k_{ad,macro}$, of propagating chains onto the control agent.[4] This coefficient is readily obtained from the slope of plots

*Corresponding authors. Website: www.macroarc.de. E-mail: (T.J.) thomas.junkers@polymer.uni-karlsruhe.de; (C.B.-K.) christopher.barner-kowollik@polymer.uni-karlsruhe.de. Telephone: (T.J.) +49 721 608 2603; (C.B.-K.) +49 721 608 5641. Fax: +49 721 608 5740.

Published on Web 07/02/2009

Scheme 1. Main Reactions of the Enhanced Spin Capturing Polymerization Process[a]

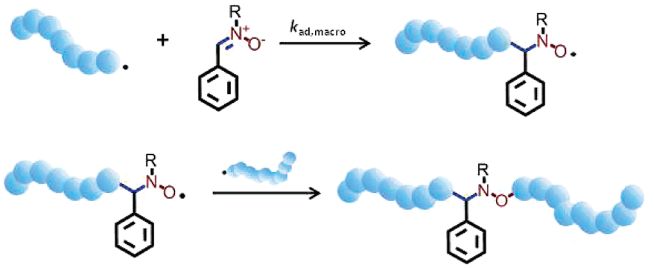

[a] The upper reaction shows the spin capturing of a macroradical, the lower one spin annihilation with a propagating chain, resulting in midchain-functionalized AA-type polymers.

of DP_n^{-1} vs $c_{Nitrone}$ and can be determined with high accuracy.[4] Knowledge of $k_{ad,macro}$ is crucial as it or the corresponding spin capture constant C_{SC} (with $C_{SC} = k_{ad,macro}/k_p$) determines whether the formed molecular weight remains constant over the course of the polymerization (ideal case, $C_{SC} = 1$) or whether a noticeable decrease of increase of M_n occurs (C_{SC} being significantly smaller or larger than unity). A question that was not addressed in the previous kinetic study was to establish to what extend the macroradical addition is in competition with initiator addition to a nitrone (see Scheme 2).

It may be envisaged that small initiator derived radicals add to a considerable rate with the surrounding nitrone molecules. Thus, a small-sized nitroxide would be formed that is subsequently available for termination. The formation of such radicals does not interfere critically with our aim of employing ESCP as a molecular weight control tool as the difference in the obtained molecular weight with the desired product is only a factor of 2, which does not constitute very significant variation in molecular weight considering the broad range of molecular weights that can generally be targeted via ESCP. The formation of such small nitroxide has, however, the effect that the alkoxyamine function is located at the chain end of the dead polymer chain.

The general ability to form midchain-functionalized polymers is, however, one of the most intriguing features of ESCP. The chains do not only carry a certain functionality (which for example can be used to *click* other chains onto it),[16,17] but the alkoxyamine function can, if purposefully designed, reinitiate NMP, thus forming ABA-type blockcopolymers, when the postpolymerization is carried out using a different monomer. However, in case the alkoxyamine function is not located in the middle of the chain—but rather on its chain end—AB-diblockcopolymers are formed that are more easily accessible when employing exclusively NMP. A situation where AB-type block copolymers are obtained predominantly occurs if initiator-derived radicals react with the nitrone as described above (or a macronitroxide terminates with an initiator-derived radical). Thus, knowledge over the ratio of midchain-functionalized vs chain-end functionalized polymers is crucial if ESCP is to be employed as a tool for (tri-) blockpolymer synthesis.

In here, we provide a comprehensive analysis of the alkoxyamine's location in the chain. The study is divided into two parts. In the first part, ESCP is modeled using the simulation software PREDICI[18] to assess the theoretical limitations of ESCP. In the second part, experimental evidence for ABA-block formation will be provided.

Experimental Section

Materials. *N-tert*-Butyl-α-phenylnitrone (PBN, Aldrich, 98%), 2,2-azobis(isobutyronitrile) (AIBN, DuPont), hydroquinones (Aldrich, 99%), *N*-isopropylacrylamide (NIPAAm, Aldrich, 97%), dimethyl formamide (DMF, Aldrich, 99.8%), toluene (Aldrich, 99.9%), and tributyltin hydride (Aldrich, 97%) were used as received. Styrene (Aldrich, 99%) was deinhibited by percolating it over a column of basic alumina.

ESCP Reactions. Polymerization samples consisted of 1.5 to 2.0 mL of styrene monomer in a glass vial containing 4×10^{-2} mol·L^{-1} of initiator and 4×10^{-2} mol·L^{-1} or 8×10^{-2} mol·L^{-1} of PBN for experiments A and B, respectively (see Results and Discussion for a description of experiments A and B). The prepared solutions were purged with nitrogen for approximately 10 min prior to reaction. Thermal polymerizations of styrene were conducted in an oil bath at 60 and 80 °C for experiments A and B respectively. An excess of hydroquinones was added to each sample after the polymerizations were stopped after 27 h to avoid any postpolymerization reactions. Residual styrene monomer was removed by evaporation in a fume cupboard and conversions were determined gravimetrically (51% and 60% for experiments A and B). The obtained polystyrene was purified via precipitation in a methanol/water (9/1 v/v) mixture (M_n = 19 000 g·mol^{-1}, PDI = 1.6 and M_n = 12 000 g·mol^{-1}, PDI = 1.5 from experiments A and B, respectively).

NMP Chain Extension. 480 mg (4×10^{-5} mol) of the polystyrene (M_n = 12 000 g·mol^{-1}, PDI = 1.5) made via ESCP was mixed with 8 mL of DMF solution containing 4.52 g (4×10^{-2} mol) of NIPAAm. The prepared solution was purged with nitrogen gas for approximately 10 min prior to reaction to remove all traces of oxygen. The chain extension experiment was then performed at 110 °C in an oil bath for 5 h. DMF was later removed from the sample under high vacuum. The reaction yielded a triblock copolymer of polystyrene-*b*-polyNIPAAm-*b*-polystyrene with M_n = 35 000 g·mol^{-1} and PDI = 1.8. The monomer conversion was determined by integration of the ^{1}H NMR spectra (in $CDCl_3$, residual peak δ = 7.26 ppm). Thereby the monomer peak chosen as reference was the vinylic peak at δ 5.4−5.7 ppm (dd, CH(*H*)=) with the integral X, which was compared to the CH peak of the isopropyl group at 3.7−4.2 ppm (m, C*H*$(CH_3)_2$) of the polymer and monomer with the integral Y. Conversion is then deduced by $(Y - X)/Y$. A 35% monomer conversion was obtained after 5 h.

Scheme 2. Competitive Addition Reactions in ESCP of Initiator Derived Radicals I• and Macroradical Chains onto the Nitrone Control Agent

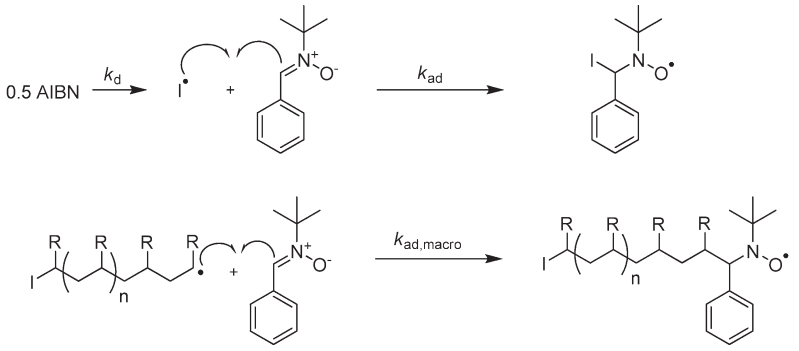

Polymer Quenching. In experiment A, to a 2 mL solution of homo polystyrene (0.19 g, 1×10^{-5} mol) made via ESCP in toluene, 0.29 g (1×10^{-3} mol) tributyltin hydride (TBTH) was added such that the ratio of polymer to quencher is 1:100. The solution was heated to 125 °C for 5 h. Under these conditions, the alkoxyamine bond is cleaved and TBTH transfers its proton to the radicals preventing recombination. As the hydride is a strong transfer agent, quantitative quenching can be assumed considering the high concentration of quencher and the relatively high temperature. The solvent was removed by evaporation in a fume cupboard before the quenched polymer was analyzed via THF−SEC. In experiment B, the polystyrene-*b*-polyNIPAAm-*b*-polystyrene triblock copolymer (0.35 g, 1×10^{-5} mol) produced via tandem ESCP-NMP reactions, was dissolved in 2 mL of DMF before adding 0.29 g (1×10^{-3} mol) TBTH. The solution was also heated to 125 °C for 5 h. DMF solvent was later removed under high vacuum.

Isolation of Diblock Copolymer after Quenching. Water was added to the quenched polymer sample for dissolving the polyNIPAAm-*b*-polystyrene diblock copolymer and the solution was filtered through a 0.45 μm membrane. The filtrate was purified by dialysis in distilled water using a dialysis membrane with molecular weight cut off of 3500 g·mol^{-1} and then dried under vacuum. Similarly for the polystyrene-*b*-polyNIPAAm-*b*-polystyrene triblock copolymer, the sample was dissolved in DMF and dialyzed in distilled water to remove residual NIPAAm monomers. For the quantitative determination of the ratio of styrene to NIPAAm contents in both the di- and triblock copolymers, integration of the ^{1}H NMR spectra were performed. The CH peak of the isopropyl group at 3.7 − 4.2 ppm (m, C*H*(CH$_3$)$_2$) of the polymer was used as the reference peak with an integrated value of 1 and the aromatic protons of the styrene at 5.7−7.4 ppm (dd, 5H, phenyl) were integrated accordingly.

Characterization by THF Size Exclusion Chromatography. For the determination of molecular weight distributions of polystyrene samples, a Shimadzu modular system, comprising an auto injector, a Polymer Laboratories 5.0 μm bead-size guard column (50 × 7.5 mm), followed by four linear PL columns (10^5, 10^4, 10^3, and 500 Å) and a differential refractive index detector using tetrahydrofuran (THF) as the eluent at 40 °C with a flow rate of 1 mL·min^{-1} was used. The SEC system was calibrated using narrow polystyrene standards ranging from 560 to $1.95 \cdot 10^6$ g·mol^{-1} (polystyrene ($K = 14.1 \times 10^{-5}$ dL·g^{-1} and $\alpha = 0.70$)).[19] Polymer concentrations were in the range 3−5 mg·mL^{-1}.

Characterization by DMAc Size Exclusion Chromatography. SEC analysis of polystyrene-*b*-polyNIPAAm-*b*-polystyrene triblock copolymer was performed in *N*,*N*-dimethylacetamide (DMAc) (0.03% w/v LiBr, 0.05% BHT stabilizer) at 50 °C (flow rate: 0.85 mL·min^{-1}) using a Shimadzu modular comprising a DGU-12A solvent degasser, an LC-10AT pump, a CTO-10A column oven, and a RID-10A refractive index detector. The system was equipped with a Polymer Laboratories 5.0 μm bead-size guard column (50 × 7.8 mm), followed by four linear PL columns (10^5, 10^4, 10^3, and 500 Å). Calibration was performed with narrow polystyrene standards ranging from 500 to 10^6 g·mol^{-1}.

Characterization by ^{1}H NMR. ^{1}H NMR spectra were recorded on a Bruker DPX spectrometer (300 MHz).

Results and Discussion

The ESCP Mechanism. The spin capturing polymerization follows a comparatively simple reaction mechanism as shown in Scheme 3. Reactions I−III plus reaction VI represent the ideal free-radical polymerization mechanism. In addition to these reaction, the nitrone addition reactions IV—addition of macroradicals $R_i^\bullet$—and V—addition of initiator derived radicals $I^\bullet$—may occur alongside the specific termination reactions VII−X. Thereby the product

Scheme 3. Reaction Scheme for Enhanced Spin Capturing Polymerization Employed for Simulating the Process in PREDICI

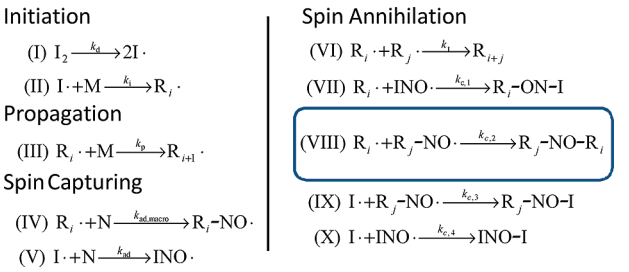

R_j−NO−R_i from reaction VIII is the anticipated reaction product of ESCP that carries the reactivatable NO−C bond in the middle of the polymer chain. Both reaction products from reactions VII and IX carry the alkoxyamine function at the chain end with the only difference being to which side the NO−C bond is facing.

As we have shown before, the weight-controlling reaction step is IV, as via this reaction chain growth is practically stopped.[3] The subsequent spin annihilation can be considered a very rapid reaction. Qualitatively, one observation that is crucial for the ESCP process can directly be made: *Any* polymerization product consists of at least two initiator fragments (each $R_i^\bullet$ was initiated by $I^\bullet$ in reaction (II)), thus the nitrone must always be used in excess to the amount of initiator to prevent full consumption of the control agent. The termination reactions VI−X are associated with different reaction rate coefficients. As styrene is a monomer that terminates particularly fast and due to the generally rapid spin annihilation of nitroxides with transient radicals, only a small variation between $k_{c,1}$ to $k_{c,4}$ is expected. Thus, whether R_j−NO−R_i is the main product of the reactions mostly depends on the concentration of $I^\bullet$ and the rate parameter k_{ad}. If $k_{ad}[I^\bullet]$ is in the same order of magnitude as $k_{ad,macro}[R_i\cdot]$ (or higher), then significant amounts of chain-end alkoxyamines will be formed. In addition, if k_{ad} is small, large numbers of $I^\bullet$ will promote reaction IX and thus also favor formation of unwanted polymer products.

PREDICI Simulations. The AIBN-initiated bulk polymerization of styrene is very well studied and a large number of rate coefficients is precisely known for a broad range of reaction conditions. For this reason, the model study presented herein was performed on this system to keep the number of unknown process parameters to a minimum. If another monomer/initiator combination was chosen, too many reaction parameters would only be known within rather broad limits, complicating the interpretation of the results from variation of the ESCP-specific reactions. Very well-known is the decomposition rate of AIBN, k_d.[20] From pulsed laser polymerization experiments, highly accurate k_p and k_t data are also available.[21,22] From our previous work on ESCP, the macroradical addition rate coefficient to PBN, $k_{ad,macro}$, is known to good accuracy and must thus not be varied in the current model study. As mentioned above, nitroxide termination can be considered very fast and close to the diffusion limit. Thus, values for k_c in the range of 10^9 L·mol^{-1}·s^{-1} may be anticipated. More exact information on the individual reactions are difficult to access. However, due to the hindered diffusivity of macroradicals, an order of $k_{c,4} > k_{c,1} \approx k_{c,3} > k_{c,2}$ with $k_{c,4} = 10^9$ L·mol^{-1}·s^{-1} should be adopted for a kinetic model. The two remaining rate parameters are k_i and k_{ad}, i.e. the two initiator-derived radical addition reactions. Fischer and Radom provided data for the addition of various types of radicals to a range of alkenes,[23] among them cyanoisopropyl radicals and

styrene. They classified radicals into elecrophilic and nucleophilic fragments and explained the variation of the individual rate coefficients of several orders of magnitude on this basis. For the AIBN fragment/styrene pair they reported a rate coefficient more than ten times larger than k_p, classifying the cyanoisopropyl radical as slightly electrophilic (the cyano group is lowering electron density at the radical site). As a consequence, radical addition becomes slower when the double bond is less electron rich. Nitrones have ionic character where the positive charge is delocalized on the double bond (see Scheme 1). Thus, at equal concentrations, AIBN fragments should add at a lower rate to nitrones than to styrene, although spin trapping is usually associated with rate coefficients in the order of 10^5-10^6 L·mol^{-1}·s^{-1}. The observation that the radical addition rates vary to such a significant extent demonstrates the importance of choosing the correct initiator system for ESCP. Oxygen centered radicals (e.g., derived from peroxide decomposition) show—for example—a much higher affinity to PBN and add more than a hundred times faster than carbon centered radicals.[24,25] It can therefore be assumed that the rate coefficient of the initiator-derived radicals is the factor that limits the ESCP process in its ability to form midchain functionalized chains. Thus, the simulation of the process should focus on these reactions. Note that the control over molecular weight is not affected.

For simulation of the ESCP styrene/AIBN system, a PREDICI model with the reactions I−X was adopted. For the purpose of this study, the reaction products of reactions VII and IX were regarded to be identical, although the reactivation by NMP at higher temperatures for both products is most likely different as in both cases the NO−C bond scission yields different types of fragments ($R_i^\bullet$ in case of reaction VII and $I^\bullet$ in case of reaction IX); however, both reaction pathways would equally result in the formation of diblocks.

Table 1. Reaction Coefficients for ESCP for the Styrene/PBN System Initiated by AIBN at 80 °C[a]

k_d[20]	k_i[23]	k_p[21]	k_{ad}	$k_{ad,macro}$[4]
1.33×10^{-4} s^{-1}	8.04×10^3	6.62×10^2	1.61×10^3 [$2k_{ad,macro}$]	8.06×10^2
k_t[22]	k_{c1}	k_{c2}	k_{c3}	k_{c4}
1.27×10^8	1×10^9	1×10^9	1×10^9	1×10^9

[a] All rate coefficients are in L mol^{-1} s^{-1} unless otherwise indicated.

For the PREDICI simulation, concentrations were employed that have been used in our previous experimental investigations (i.e., $c_{Sty} = 10$ mol·L^{-1}, $c_{PBN} = 0.1$ mol·L^{-1}, $c_{AIBN} = 0.05$ mol·L^{-1}) and a reactor temperature of 80 °C (the monomer concentration was idealized to allow for easier comparison of monomer concentration with other low-molecular reactants, the actual bulk concentration of styrene at 80 °C is slightly lower). As described above, rate coefficients for initiator decomposition, propagation, termination and addition of macroradicals to the nitrone are available in the literature.[4,20−22] Initially, all nitroxide combination rate coefficients were set to 10^9 L·mol^{-1}·s^{-1}. The addition rate coefficient of the initiator-derived radicals to PBN was set at twice the value of $k_{ad,macro}$. Numbers for all rate coefficients used in the model (extrapolated to 80 °C) are collated in Table 1.

Two simplifications were made in the model: Conventional termination was set to exclusively occur via combination, which may not be fully representative of what is occurring in the real polymerization system. We will, however, show below that conventional termination only plays a small role in ESCP. In a further simplification, the initiator efficiency, f, is set to unity. Changing the efficiency to realistic values (with f being close to 0.7) would, however, only have a slight influence on the process.

Figure 1 depicts the simulation outcome of the model on the basis of the above-described parameters. The simulation was carried out for a reaction time of 10 h, which is the point in time where the initiator is almost quantitatively decomposed. Under the adopted reaction conditions, a monomer conversion of 40% is reached and about 50% of the nitrone is consumed (based on a 2:1 ratio of PBN:AIBN).

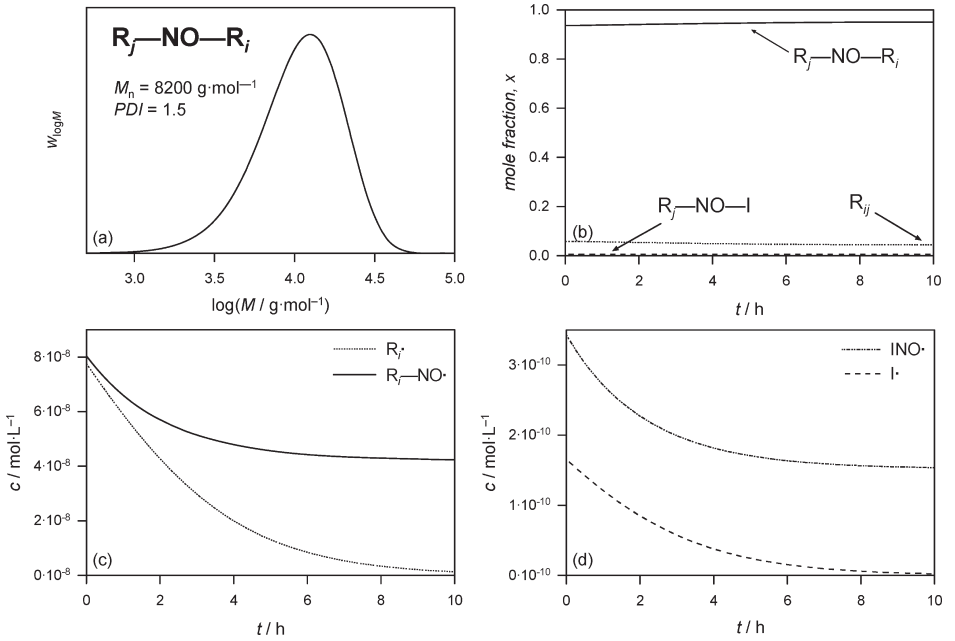

Figure 1. Simulation results for an ESCP of styrene mediated by the nitrone PBN. The polymerization was simulated for 80 °C and a reaction time of 10 h on the basis of the reaction set given in Scheme 3 and the rate coefficients provided in Table 1. (a) Depicts the molecular weight distribution of the midchain functionalized polymer, (b) gives individual concentrations of the reaction products over the course of polymerization. (c) Displays the macroradical concentrations and (d) the small radical concentrations as a function of reaction time.

The observation that 50% of the nitrone is consumed comes as no surprise as each initiated chain incorporates a nitrone moiety. As can be seen, the composition of the reaction product does not change significantly over time (and thus with monomer conversion). It is expected that the situation would not be changed if polymerization conditions are chosen to allow for higher monomer conversions (by choosing a different type of initiator that decomposes at higher temperatures and is not quantitatively reacted after 10 h). On the upper left of Figure 1, the molecular weight distribution of the midchain functionalized polymer product is shown. As a result of the specific nitrone concentration, a number average molecular weight of $M_n = 8200\ g \cdot mol^{-1}$ is obtained after 10 h of reaction time (at the initial stages of the polymerization, the molecular weight is close to $8000\ g \cdot mol^{-1}$; the increase occurs due to C_{SC} being slightly larger than unity). On the upper right side, the mole fraction profiles for the three polymer products are shown. The forth potential product, INO−I is not shown as its concentration is at all times 5 orders of magnitude smaller than that of the product R_j−NO−R_i and hence can be neglected. Parts c and d of Figure 1 show the individual concentrations of the various radical species present during the reaction. As can be seen, the midchain-functionalized polymer is by far the most abundant species formed during the whole course of the reaction, while chain-end functionalized alkoxyamines does not occur in significant quantities; the only side product is the conventional termination product. However, even these R_{ij} only contributes not more than 5% of the total product. Thus the situation—as simulated under the chosen conditions—can be regarded to be a good reaction outcome with respect to the desired formation of midchain-functionalized polymer. It is clear that 100% functionalization is not achievable in any radical process, and in fact, any ESCP resulting in more than 90% of the desired material may be seen as successful (keeping in mind that also polymer made via RAFT polymerization—provided optimum conditions are chosen—usually contains about 5% dead polymer)[26] and even 80% functionalization may be acceptable, when considering these efficiencies that are typically reached in, e.g., star polymer syntheses via living radical processes.[27] Any specific polymer product species that constitutes more than approximately 85% of the total material formed in a reaction will in the framework of this work be considered to be uniform.

The kinetic situation described above thus resembles an optimum ESCP system in which not only molecular weight control is maintained, but also good control over the molecular functionality is observed. However, the kinetics of the process may vary when another initiator is used and/or if the type of monomer is changed. In addition—and depending on the structure of the employed nitrone—the termination reaction may be hindered due to steric reasons. In such a case, the formation of the desired R_i−NO−R_j structure would be less favored. Therefore, simulations were carried out where $k_{c,2}$ was varied to establish under which boundaries ESCP still yields polymers with an acceptable uniformity.

Figure 2 shows the mole fractions of the R_i−NO−R_j polymer compared to the fractions of the other two reaction products as a function of $k_{c,2}$. In this specific case, $k_{c,1}$ and $k_{c,3}$ were set to $5 \times 10^8\ L \cdot mol^{-1} \cdot s^{-1}$ (and thus a factor of 2 lower than in the previous simulation) as it can be expected that macromolecules terminate not as rapidly as small radicals. $k_{c,4}$ remained at $10^9\ L \cdot mol^{-1} \cdot s^{-1}$; any higher value did not appear to be reasonable, as termination rate coefficient of $10^9\ L \cdot mol^{-1} \cdot s^{-1}$ are among the highest values

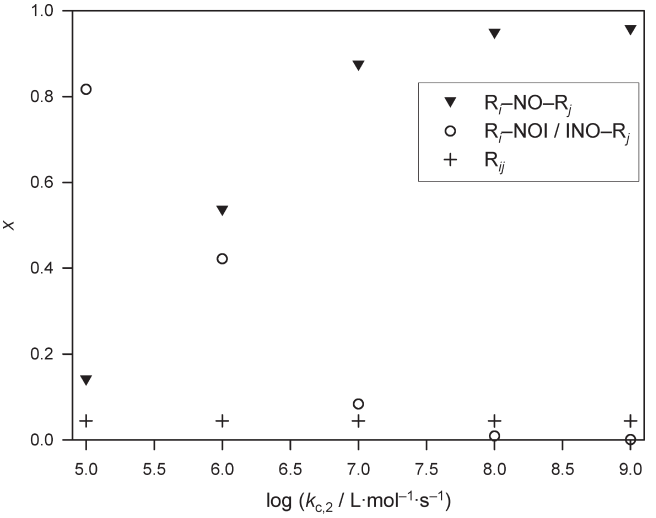

Figure 2. Variation in the individual mole fractions of polymer products with the combination rate of macronitroxides with free propagating chains.

measured for these reactions. Inspection of Figure 2 indicates that the mole fraction of conventional termination product is largely uninfluenced by the termination level of the macronitroxides. A large variation in the fraction of R_i−NO−R_j as well as R_i−NOI is observed when $k_{c,2}$ is decreased. When $k_{c,2}$ is in the same order of magnitude as the other termination rate coefficients, the mole fraction of the desired midchain-functionalized product is well above 90%. At $k_{c,2} = 10^7\ L \cdot mol^{-1} \cdot s^{-1}$ sufficient amounts, still reasonable above 80%, of the desired product are still formed, but when the rate coefficient is further decreased, a severe reduction is observed and the reaction product cannot be regarded to be of midchain-fuctionalized material anymore. Still, the results from the simulations as shown in Figure 2 show that the formation of the target polymer with the alkoxyamine function being located in the middle of the chain is mostly not affected by the individual termination rates as the kinetic limits in which a successful experiment may be assumed are relatively broad and a macronitroxide termination that is over 1 order of magnitude slower than conventional termination is unlikely. In addition, the assumption of a comparatively small $k_{c,2}$ at the same time with an unchanged large $k_{c,1}$ and $k_{c,3}$ is also no realistic scenario. However, to err on the side of caution, all further simulations were carried out with $k_{c,2} = 10^8\ L \cdot mol^{-1} \cdot s^{-1}$ and the results shown below must always be seen as the extreme lower limit of what is achievable from the viewpoint of the termination level.

A further important kinetic parameter that needs to be tested is the rate coefficient for the addition of primary radicals onto the controlling nitrone. This reaction competes with monomer addition to primary radicals, i.e. the initiation step and both corresponding rate coefficients may be seen as a pair of parameters. Thus, in Figure 3, the mole fraction of R_i−NO−R_j is shown as a function of the logarithm of k_{ad} over k_i. In the styrene/PBN/AIBN system, the initiation rate is known. In most other systems, however, this rate coefficient is not as readily available and it is known that k_i can change significantly with the type of initiator and monomer used. From spin trapping experiments it is known that k_{ad} can vary over several orders of magnitude. For the nitrone class, addition rate coefficients of up to $10^8\ L \cdot mol^{-1} \cdot s^{-1}$ have been determined for several small transient radicals.[24] It is therefore important to perform the variation of the

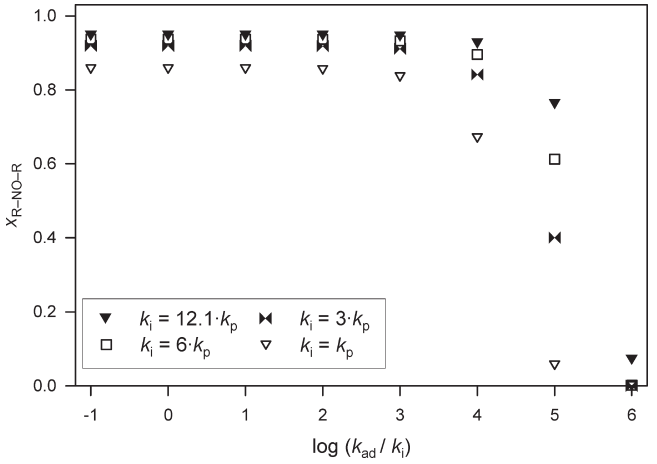

Figure 3. Decline in midchain-functionalized polymer content with increasing ratios of the small radical addition rate coefficient over the initiation rate coefficient at different ratios of k_i/k_p. k_p was constant in all simulation at a value of 663 $L \cdot mol^{-1} \cdot s^{-1}$.

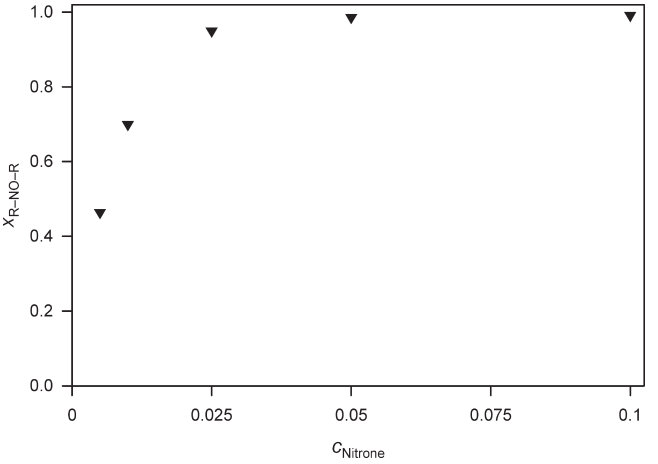

Figure 4. Variation of midchain-functionalized polymer content with nitrone concentration and constant initiator concentration (5×10^{-3} $mol \cdot L^{-1}$).

addition rate coefficient also under varying ratios of k_i over k_p. Consequently, Figure 3 shows values for four discrete values of k_i/k_p starting with a factor of 12.1 (the value determined for styrene/AIBN) down to k_i being equal to k_p. In all simulations carried out in this context, k_p was kept constant at 663 $L \cdot mol^{-1} \cdot s^{-1}$.

The primary radical concentration is very small at all times during polymerization. It should be noted that all simulations were carried out without primary radical termination with its own kind or with propagating radical chains. Thus, the simulation results presented in the following display an upper limit as in real systems the respective radical polymerization will always be smaller than anticipated here. Thus, in order to find significant changes in the product spectrum, very high values of k_{ad} compared to k_i must be assumed as the monomer concentration will in most cases be several magnitudes larger than the nitrone concentration, thus favoring the classical initiation reaction. This result is immediately seen in Figure 3: For all ratios of k_i/k_p mostly unchanged product compositions are found at least from $-1 < \log(k_{ad}/k_i) < 3$ which mostly accounts for the difference in concentrations of the reaction partners. Only when very large values for k_{ad} are assumed (with the minimum values close to 10^7 in the most unfavorable case) a drastic decrease in x_{R-NO-R} can be observed. However, in the case of k_i being much larger than k_p, a k_{ad} value of close to 10^9 $L \cdot mol^{-1} \cdot s^{-1}$ and thus close to the diffusion limit must be assumed to bring the desired product ratio below 90%. Thus, as long as no nitrone which displays a particularly rapid primary radical addition in combination with a relatively small chain growth initiation rate, the size of k_{ad} appears to be unproblematic for the success of R_i-NO-R_j formation by ESCP.

Independent from the variation of the addition rate, Figure 3 shows another interesting result. When k_i is reduced compared to k_p, the mole fraction of the midchain functionalized polymer that is achievable even at the most favorable k_{ad} decreases. This reduction is not associated with the competition of primary radical addition but rather with termination of macronitroxides with the surrounding primary radicals, as the number of primary initiating radicals available for termination increases when k_i is decreased. Thus, for an optimum ESCP, an initiator with a high initiation rate should always be chosen. Detrembleur et al. have performed reactions employing PBN for styrene polymerization in the context of the in situ NMP method[28] and they found chain-end functionalized polymers only when they used a peroxide as an initiator. This observation is in very good agreemement with the above simulations as peroxides generally are—compared to azoinitiators—associated with low k_i while k_{ad} remains large.

Figure 4 shows the influence of the nitrone concentration on the reaction product. The figure covers a variation of $c_{Nitrone}$ from 0.01 to 0.1 $mol \cdot L^{-1}$. In all cases (and at even lower $c_{Nitrone}$), good control of the overall molecular weight is experimentally found.[4] However, the simulation shows that long before control over molecular weight is lost (all simulation carried out in this work, even in the most extreme cases, show good overall control over molecular weight), the homogeneity of the product spectrum is lost. At concentrations above 0.025 $mol \cdot L^{-1}$ more than 90% desired product is expected. Such nitrone concentrations (in the styrene/PBN system) still allows for molecular weights of about 50 000 $g \cdot mol^{-1}$. However, when the nitrone concentration is further reduced to target larger polymer chains, x_{R-NO-R} starts to decrease rapidly. Of course, the exact limit from where on such decrease may be observed will largely depend on the full kinetics of the system and under assumption of other addition and termination rates, the depicted picture might change. Nevertheless, Figure 4 shows the importance of using comparatively larger nitrone concentrations when ESCP is to be used for the construction of more complex macromolecular architectures.

An influence that has not been tested yet is the radical concentration. Generally, in ESCP, the initiator concentration has only little influence on the molecular weight that is formed during polymerization. However, the overall number of radicals does of course influence the termination reaction. Therefore, simulations have been carried out under assumption of various reaction temperatures, which directly results in a variation of the associated radical concentrations. Generally, the impact of temperature (and thus changing radical concentration) is relatively small. Even at temperatures of close to 100 °C, significantly more than 80% of all polymer chains are midchain-functionalized. As bond cleavage of the alkoxyamine starts to become a significant reaction at these temperatures, superimposing an NMP process on the ESCP, no higher temperatures need to be considered as any reaction performed at higher temperatures would be closer to a NMP reaction than actual ESCP.

From the simulations it may thus be concluded that the formation of midchain-functionalized material, i.e. polymers

Scheme 4. Two Strategies Followed To Test for Formation of Midchain Functionalized Polymers Made via ESCP

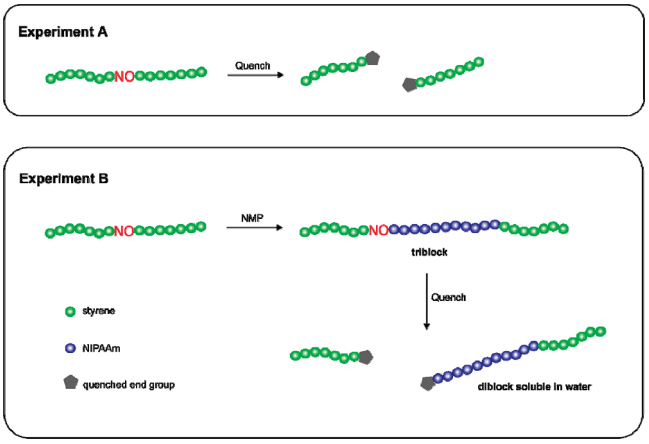

that can be transformed into ABA-type triblockcopolymers by subsequent NMP, is the dominant reaction pathway. Success of the polymerizations with respect to the midchain functionalization is mostly dependent on the choice of the initiator/nitrone combination (to tune the ratio of k_{ad}/k_i). Formation of dead chains does not play a significant role as is to be expected in a system where molecular weight is well controlled. Formation of reactivatable chains which carry the alkoxyamine function at the chain end (either capped with the NO−C bond by an initiator fragment (reaction IX) or by the whole polymer chain, (reaction VII) does occur and can become dominant under certain extreme kinetic scenarios as described above. Under most conditions however, 90% and above of the formed polymer consists of midchain-functionalized material and the formation of end-capped polymers can be regarded to be a relatively insignificant side reaction. However, it must be stated that the above simulations were carried out on a styrene/AIBN system. If the monomer is changed to a system that exhibits very different termination and propagation behavior, the situation might vary to some degree. As the nitrone addition is—most likely—correlated with the propagation rate[29] and the radical combination rates probably scale with the termination rate coefficient of two macroradical chains, it can be assumed that the results would not be changed dramatically. The worst case scenario would be a monomer that propagates very slowly but at the same time terminates at relatively high rates. Such kinetic situation would then favor conventional termination over the ESCP specific reactions. However, such a monomer would be difficult to polymerize anyway.

Experimental Support. Although the PREDICI simulations demonstrate that in a relatively broad kinetic range ESCP yields polymers with the vast majority of chains carrying the alkoxyamine functionality in the middle of the chain, further experimental proof was sought to verify the simulations. In order to achieve this aim, two strategies were followed that are illustrated in Scheme 4. In both approaches the ability to cleave the alkoxyamine functionality with subsequent quenching of the resulting radical macroradical fragments was employed. Such a strategy allows for the individual characterization of the blocks on both sides of the NO−C linker.

In the first test, shown in the scheme as experiment A, homopolymer made from styrene/AIBN/PBN was directly subjected to quenching of the chains by treatment of the sample with tributyltin hydride at 125 °C. Under these conditions the NO−C bond is cleaved and the radical

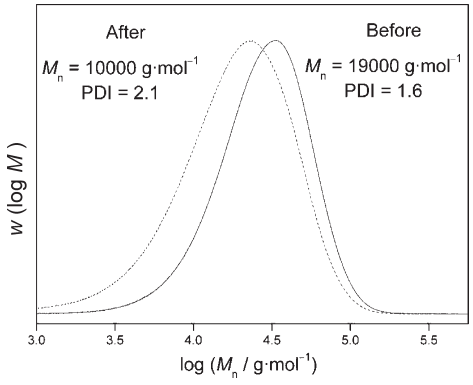

Figure 5. Experimental molecular weight distribution of polystyrene made from ESCP ("before") and the distribution of the same polymer "after" quenching the chains with tributyltin hydride at 125 °C.

fragments are annihilated by the tin hydride leaving two dead chains that cannot function anymore in an NMP or ESCP process.

The effect of the quenching experiment A is illustrated in Figure 5. The ESCP-made polymer before the quenching experiment had an average molecular weight of about 19 000 g·mol^{-1} and a polydispersity index, PDI of 1.6 which is in line with the observations made above in the simulations (see Figure 1a—however, note that an M_n of 8200 g·mol^{-1} is obtained in the simulations when the input $c_{Nitrone}$ is set at 0.1 mol·L^{-1} whereas in experiment A, 0.04 mol·L^{-1} of PBN was used and therefore a higher M_n is obtained). Thus, the polymer used for experimental proof of the validity of our simulations marks an upper boundary. Any higher nitrone concentration (and thus synthesis of smaller ESCP product) would promote the formation of midchain-functionalized polymer as is demonstrated in Figure 4. Only at lower nitrone concentrations will the effectiveness of the ESCP process decline, and a polymer that was not suitable for carrying out experiments A and B would be obtained.

Because ESCP yields almost exclusively polymers that are generated by a combination of two chains, the resulting distribution resembles the MWD of a polymer made by conventional free-radical polymerization that exclusively terminates via combination. Thus, a PDI of almost 1.5 is observed due to combination statistics. After the polymer sample is quenched the most immediate observation is the reduction in molecular weight to 10 000 g·mol^{-1}, which is approximately half the size of the polymer before chain scission. This reduction in average molecular weight by a factor of almost 2 indicates that the linking alkoxyamine bridge between the two resulting chains was located in the middle of the chain for the vast majority of all individual polymer species. If a significant number of the ESCP-derived chains would have had the functionality at the chain end, then a lower overall mass reduction should have been observed. For chain-end functionalized polymers quenching would result in a chain-end modification with no significant reduction in molecular weight. Concomitantly with the reduction in average chain size, the PDI of the quenched polymer increased to 2.1, which is, within experimental accuracy, the limit for a polymer distribution generated via disproportionation (that is characterized by the PDI = 2 of a Schulz−Flory distribution). The quenched distribution hence resembles the radical distribution during the polymerization before linking of two radical chains via spin capturing has taken place.

Both the reduction of the molecular weight by a factor of 2 as well as the increase in PDI to 2.1 independently proof that

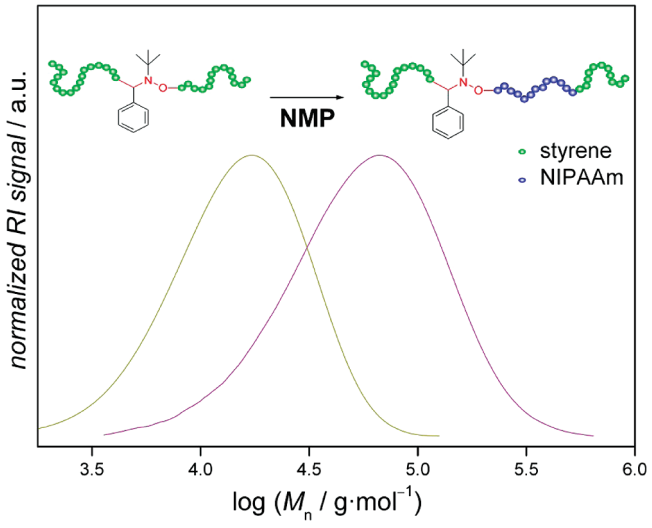

Figure 6. Experimental molecular weight distributions of ESCP polymer before and after chain insertion of NIPAAm via tandem ESCP-NMP reactions.

the alkoxyamine functionality is located in midchain position. The observation that the initial molecular weight is slightly smaller than would be expected from the quenched size distribution (in a thought experiment, polymer of 20 000 g·mol^{-1} would be formed if the quenched distribution would be converted back into an ideal combination distribution) is explained by the low but yet noticeable extend to which conventional termination between two uncaptured radical chains occurs. As the simulations have shown, few percent of dead polymer material is expected even under ideal conditions for the ESCP process (a circumstance that is however true for all radical polymerizations, including living/controlled polymerization techniques). As styrene primarily terminates via combination,[30] a small fraction of polymer is generated that cannot be cleaved in the quenching process and that shifts the average molecular weight to slightly larger values. On a side note, it should also be mentioned that the observed change in the MWD from the quenching not only gives strong indication for the proposed structure of the ESCP-made polymer but also for a quantitative quenching of chains by the chosen reaction procedure.

Another approach to analyze the alkoxyamine location is to use the same quenching method on ESCP polymers that were chain extended via NMP, denoted as experiment B in Scheme 4. As a result from such an experiment, two subdistributions of disparate average length should become observable. One distribution should reflect the chain distribution of chains that initially added the nitrone to form a macronitroxide—the Schulz−Flory distribution with PDI close to 2 and with approximately half the size of the original ESCP polymer. This subdistribution does not change its size during NMP as the C−NO bond is thermally stable and does not cleave. The second distribution, however, should consist of chains that are substantially larger. While the chains that were attached on the NO−C side of the alkoxyamine originally had the same distribution as the chains attached via the C−NO bond, a substantial increase in chain length can be achieved by the NMP process which makes this distribution distinguishable from each other.

Figure 6 depicts the molecular weight distribution from polystyrene that was chain-extended by *N*-isopropylacrylamide (NIPAAm). To allow for a clear distinction of the different distributions after quenching, the molecular weight of the polymer was substantially increased from

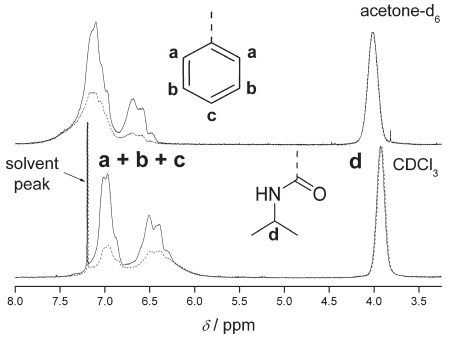

Figure 7. NMR spectra of the di- (dotted line) and triblock (full line) structures in two different solvents. All spectra were normalized on the signal according to the proton at the isopropyl group of NIPAAm.

Table 2. Integration Results in the Aromatic Region for the NMR Spectra shown in Figure 7

solvent	triblock	diblock	ratio of integrals
acetone-d_6	2.76	1.40	1.97
$CDCl_3$	2.82	1.46	1.93

12 000 g·mol^{-1} to approximately 35 000 g·mol^{-1}. Using the water-soluble NIPAAm for the formation of the triblockstructure has the advantage that the water-insoluble polystyrene is converted into amphiphilic material. Thus, after quenching of the triblocks with tributyltin hydride, a water-soluble fraction containing a polyNIPAAm block and pure hydrophobic polystyrene is formed. A separation of both fractions can thus be achieved by dissolving the amphiphilic diblock in water with subsequent filtering of the sample. As the polyNIPAAm-*co*-polystyrene diblock is also oil-soluble, the isolation of the pure polystyrene block is not possible.

Due to the changed SEC elution profile of diblock copolymers compared to their parent homopolymers it is difficult to assess by how much the average chain length was reduced in the quenching and separation procedure. Thus, the NIPAAm copolymer was analyzed via NMR spectroscopy. With regards to experiment B, the chain-extended polymer before quenching is referred to as triblocks and the blockcopolymer that is formed upon quenching is referenced as diblocks.

NMR spectra of the isolated triblocks and the diblocks are shown in Figure 7. To asses their individual quantities, the spectral region of the aromatic protons was used (as a measure for styrene) as well as the peak resulting from the tertiary proton of the isopropyl moiety on the NIPAAm units. The spectra were normalized on the isopropyl proton. As the $CHCl_3$ peak overlaps with the aromatic signal of the styrene units (see lower part of the figure), spectra have also been recorded using acetone-d_6 as solvent to verify the results from integrating the spectra taken in chloroform-*d*. It should be noted that in both cases, the signal of the NH-proton might contribute to the integration of the aromatic region, resulting in an overestimation of the polystyrene content in the polymer. Such error in the integration will, however, systematically be followed by a decrease of the ratio of integrals, and the values given in Table 2 must be seen as a lower limit.

The integration results are given in Table 2. If the unquenched sample had consisted of almost pure triblockcopolymer with only insignificant amounts of nonextendable homopolystyrene or diblocks formed from styrene chains that had an alkoxyamine-moiety at the chain end, then ratios of 2 should be found when comparing the styrene signal of

the triblocks and the diblocks. Inspection of Table 2 indicates that values well exceeding 1.9 are found. This result is in very close agreement with the simulations and the other quenching experiment shown in Figure 5. Again, formation of significant amounts of side-products or chain-end functionalized material during the ESCP process can be largely excluded. It should be noted that this result again supports the quantitative nature of the quenching procedure that was already concluded from the resulting MWDs in the context of Experiment A. If quenching was not quantitative, residual triblock copolymer would be left in the sample and smaller ratio of the integrals should be observed.

Conclusions

The formation of a polymer that is functionalized with a potentially NMP-active alkoxyamine moiety from the enhanced spin capturing polymerization technique has been confirmed via simulation and experiment. Modeling of ESCP under a broad selection of kinetic scenarios shows that the process is relatively robust and delivers a chemically and structurally homogeneous product when the reaction conditions (mostly choice of initiator or type and concentration of the nitrone) are judiciously chosen.

The simulation results were confirmed by experiments where the parity of average chain lengths on both sides of the alkoxyamine function was proven by size exclusion chromatography and further supported by NMR spectroscopy. While the location of the alkoxyamine in the ESCP-derived polymer has only little or no influence on the weight-controlling abilities of ESCP, is has profound effect on the structure of the copolymers that are formed in tandem ESCP-NMP reactions as only the midchain-functionalized polymer allows for the formation of ABA-type triblockcopolymers in the subsequent NMP process.

Acknowledgment. C.B.-K. acknowledges funding from the Karlsruhe Institute of Technology (KIT) in the context of the Excellence Initiative for leading German universities supporting the current project. C.B.-K. and E.H.H.W acknowledge support from UNSW central funding in the context of an Australian Research Council Discovery Grant to C.B.-K. for a postgraduate scholarship (to E. H. H. W.). Additional support from the Fonds der Chemischen Industrie to T. J. is also gratefully acknowledged. The authors would like to note and thank the reviewer of our previous contribution,[3] who suggested to probe the ABA triblock copolymer formation efficiency via the herein described quenching experiment A.

References and Notes

(1) Barner, L.; Davis, T. P.; Stenzel, M. H.; Barner-Kowollik, C. *Macromol. Rapid Commun.* **2007**, *28*, 539–559.
(2) Matyjaszewski, K. *Prog. Polym. Sci.* **2005**, *30*, 858–875.
(3) Wong, E. H. H.; Junkers, T.; Barner-Kowollik, C. *J. Polym. Sci. Polym. Chem.* **2008**, *46*, 7273–7279.
(4) Wong, E. H. H.; Stenzel, M. H.; Junkers, T.; Barner-Kowollik, C. *J. Polym. Sci. Polym. Chem.* **2009**, *47*, 1098–1107.
(5) Ah Toy, A.; Chaffey-Millar, H.; Davis, T. P.; Stenzel, M. H.; Izgorodina, E. I.; Coote, M. L.; Barner-Kowollik, C. *Chem. Commun.* **2006**, 835–837.
(6) Chaffey-Millar, H.; Izgorodina, E. I.; Barner-Kowollik, C.; Coote, M. L. *J. Chem. Theory Comput.* **2006**, *2*, 1632–1645.
(7) Junkers, T.; Stenzel, M. H.; Davis, T. P.; Barner-Kowollik, C. *Macromol. Rapid Commun.* **2007**, *28*, 746–753.
(8) Günzler, F.; Junkers, T.; Barner-Kowollik, C. *J. Polym. Sci. Polym. Chem.* **2009**, *47*, 1864–1876.
(9) Junkers, T.; Wong, E. H. H.; Szablan, Z.; Davis, T. P.; Stenzel, M. H.; Barner-Kowollik, C. *Macromol. Rapid Commun.* **2008**, *29*, 503–510.
(10) Hawker, C. J.; Bosman, A. W.; Harth, E. *Chem. Rev.* **2001**, *101*, 3661–3688.
(11) Fischer, H. *Chem. Rev.* **2001**, *101*, 3581–3610.
(12) Sciannamea, V.; Jerome, R.; Detrembleur, C. *Chem. Rev.* **2008**, *108*, 1104–1126.
(13) Sciannamea, V.; Catala, J. M.; Jerome, R.; Detrembleur, C. *J. Polym. Sci., Polym. Chem.* **2007**, *45*, 1219–1235.
(14) Sciannamea, V.; Guerrero-Sanchez, A.; Schubert, U. S.; Catala, J. M.; Jerome, R.; Detrembleur, C. *Polymer* **2005**, *46*, 9632–9641.
(15) Sciannamea, V.; Catala, J.-M.; Jerome, R.; Jerome, C.; Detrembleur, C. *J. Polym. Sci., Polym. Chem.* **2009**, *47*, 1085–1097.
(16) Kolb, H. C.; Finn, M. G.; Sharpless, K. B. *Angew. Chem., Int. Ed.* **2001**, *40*, 2004–2021.
(17) (a) Sinnwell, S.; Inglis, A. J.; Davis, T. P.; Stenzel, M. H.; Barner-Kowollik, C. *Chem. Commun.* **2008**, 2052–2054. (b) Inglis, A. J.; Sinnwell, S.; Stenzel, M. H.; Barner-Kowollik, C. *Angew. Chem.* **2009**, *48*, 2411–2414.
(18) (a) Wulkow, M. *Macromol Theory Simul.* **1996**, *5*, 393. (b) Wulkow, M.; Busch, M.; Davis, T. P.; Barner-Kowollik, C. *J. Polym. Sci., Polym. Chem.* **2004**, *42*, 1441–1448.
(19) Strazielle, C.; Benoit, H.; Vogl, O. *Eur. Polym. J.* **1978**, *14*, 331–334.
(20) Van Hook, J. P.; Tobolsky, A. V. *J. Am. Chem. Soc.* **1958**, *80*, 779.
(21) Buback, M.; Gilbert, R. G.; Hutchinson, R. A.; Klumpermann, B.; Kuchta, F. D.; O'Driscoll, K. F.; Russell, G. T.; Schweer, J. *Macromol. Chem. Phys.* **1995**, *196*, 3267–3280.
(22) Buback, M.; Kuchta, F. D. *Macromol. Chem. Phys.* **1997**, *198*, 1455–1480.
(23) Fischer, H.; Radom, L. *Angew. Chem., Int. Ed.* **2001**, *40*, 1340–1371.
(24) Kemp, T. J. *Prog. React. Kinet. Mech.* **1999**, *24*, 287–358.
(25) Grishin, D. F.; Semenycheva, L. L.; Kolyakina, E. V. *Russ. J. Appl. Chem.* **2001**, *74*, 494–497.
(26) Moad, G.; Barner-Kowollik, C. In *Handbook of RAFT Polymerization*; Barner-Kowollik, C., Ed.; Wiley-VCH: Weinheim, Germany, 2007; pp 51−104.
(27) Inglis, A.; Sinnwell, S.; Davis, T. P.; Barner-Kowollik, C.; Stenzel, M. H. *Macromolecules* **2008**, *41*, 4120–4126.
(28) Detrembleur, C.; Sciannamea, V.; Koulic, C.; Claes, M.; Hoebeke, M.; Jerome, R. *Macromolecules* **2002**, *35*, 7214–7223.
(29) An increase of the propagation rate coefficient by orders of magnitude is most likely associated with an increase of the addition rate to a similar extent. Indeed, we have experimentally observed such a behavior for $k_{ad,macro}$ in our previous work.[3,4]
(30) Zammit, M. D.; Davis, T. P.; Haddleton, D. M.; Suddaby, K. G. *Macromolecules* **1997**, *30*, 1915–1920.